Development of an *in situ* polarization-dependent total-reflection fluorescence XAFS measurement system

Wang-Jae Chun,[a]† Yasuhiro Tanizawa,[a] Takafumi Shido,[a] Yasuhiro Iwasawa,[a] Masaharu Nomura[b] and Kiyotaka Asakura[c]*

[a]Department of Chemistry, Graduate School of Science, The University of Tokyo, 7-3-1 Hongo, Bunkyo-ku, Tokyo 113-0033, Japan, [b]Photon Factory, Institute of Material Structure Science, Oho, Tsukuba 305-0801, Japan, and [c]Catalysis Research Center, Hokkaido University, Kita 11 Nishi 10, Kita-ku, Sapporo, 060-0811, Japan. E-mail: askr@cat.hokudai.ac.jp

An *in situ* polarization-dependent total-reflection fluorescence X-ray absorption fine structure (PTRF-XAFS) spectroscopy system has been developed, which enables PTRF-XAFS experiments to be performed in three different orientations at various temperatures (273–600 K) and pressures (10^{-10}∼760 torr). The system consists of a measurement chamber and a preparation chamber. The measurement chamber has a high-precision six-axis goniometer and a multi-element solid-state detector. Using a transfer chamber, also operated under ultra-high-vacuum conditions, the sample can be transferred to the measurement chamber from the preparation chamber, which possesses low-energy electron diffraction, Auger electron spectroscopy and X-ray photoelectron spectroscopy facilities, as well as a sputtering gun and an annealing system. The *in situ* PTRF-EXAFS for Cu species on TiO_2 (110) has been measured in three different orientations, revealing anisotropic growth of Cu under the influence of the TiO_2 (110) surface.

Keywords: polarization-dependent total-reflection fluorescence; metal–substrate interface; Cu/TiO_2 catalyst.

1. Introduction

Most industrial catalysts are used in the form of supported-metal catalysts. The role of the support is not only to disperse the active sites but also to modify the catalytic properties through so-called 'metal–support interactions'. Although a number of concepts have been proposed to explain the metal–support interaction, lack of accurate knowledge about the interface structures and the bonding features between active metal sites and support surfaces inhibits a full understanding of the essence of the metal–support interaction.

Extended X-ray absorption fine structure (EXAFS) spectroscopy is one of the most powerful techniques currently used to study the structure of supported catalysts (Koningsberger & Prins, 1988; Iwasawa, 1996). In order to determine the interface structure in a supported catalyst, EXAFS has been applied to model catalysts in which small metal particles are deposited on powder oxides (van Zon *et al.*, 1984; Martens *et al.*, 1988; Koningsberger & Gates, 1992; Asakura *et al.*, 1985; Koningsberger *et al.*, 1996). However, careful interpretation and analysis are required to elucidate the interface structures because the results derived from the usual EXAFS are averaged in all directions and the contribution from the interface structure is often weaker than that from the metal–metal interaction in the metal particles.

EXAFS has a polarization dependence expressed as

$$\chi(k) = 3 \sum \cos^2(\theta_i)\, \chi_i(k), \qquad (1)$$

where $\chi(k)$, θ_i and $\chi_i(k)$ are an EXAFS oscillation, an angle between the ith bond and the polarization vector of the incident X-ray, and an EXAFS oscillation accompanying the ith bond, respectively. Hence, equation (1) indicates that if one can use a flat substrate with active metal species deposited thereon and set the sample surface parallel to the electric polarization vector, one can obtain the interface structure selectively.

In order to investigate the structure of the metal species dispersed on the flat substrate, we have developed polarization-dependent total-reflection fluorescence X-ray absorption fine structure (PTRF-XAFS) spectroscopy (Asakura *et al.*, 1993, 2000; Shirai & Iwasawa, 1996). The total-reflection fluorescence mode is necessary to obtain EXAFS of the surface species when the coverage of the surface species is less than one monolayer (Heald *et al.*, 1984, 1988; Chen & Heald, 1993). We have applied the method to Co oxide on α-Al_2O_3 (0001), Cu oxide on α-quartz (0001), Pt_4 clusters on α-Al_2O_3 (0001), and Mo oxide on rutile TiO_2 (110) (Shirai *et al.*, 1992; Shirai, Asakura & Iwasawa, 1994; Shirai, Inoue *et al.*, 1994; Asakura *et al.*, 1997; Chun

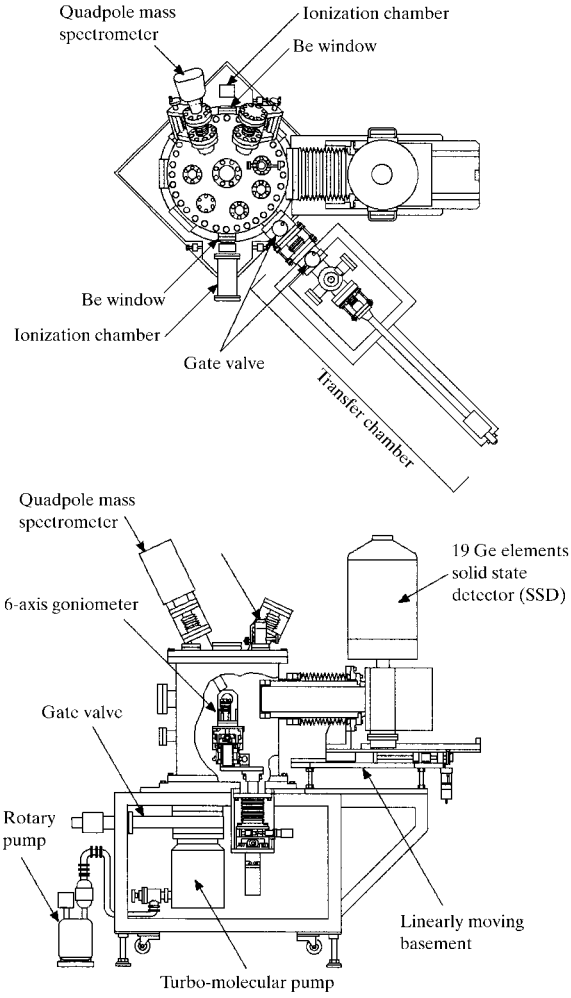

Figure 1
The *in situ* polarization-dependent total-reflection fluorescence (PTRF) measurement chamber with the sample-transfer chamber.

† Present address: Center for Analytical Chemistry and Science, Inc., 8-3-1, Chu-o, Ami, Inashiki, Ibaraki 300-0332, Japan.

et al., 1998). We have found that Pt deposited on α-Al_2O_3 (0001) has a one-atomic-layer structure with Pt—O(Al) = 0.220 nm (Asakura *et al.*, 1997). In the Mo oxide on TiO_2 (110), a dimer structure is formed with an Mo—Mo bond perpendicular to the (001) direction and Mo—O(Ti) and Mo—Ti distances of 0.220 and 0.295 nm, respectively (Chun *et al.*, 1998). We have also developed an *in situ* PTRF-XAFS chamber suitable for catalyst samples investigated under reaction conditions (Shirai *et al.*, 1995). However, it was difficult to install a heavy multi-element solid-state detector (SSD) for the fluorescence detection or an LEED (low-energy electron diffraction)–AES (Auger electron spectroscopy) instrument for surface characterization, because the position and orientation of the whole chamber needed to be adjusted to obtain the total-reflection conditions.

In this paper, we report the design and the performance of a newly built *in situ* system for PTRF-XAFS measurements. The system had to realise the following concepts.

(i) *In situ* measurements under various temperatures and pressures should be possible.

(ii) *In situ* adjustments of the total-reflection conditions and the sample orientations should be possible.

(iii) A multi-element SSD should be installed.

(iv) The chamber should be compact enough to be set in any XAFS beamline hutch in the Photon Factory.

(v) Combination with other surface-science techniques (LEED, AES) should be facilitated.

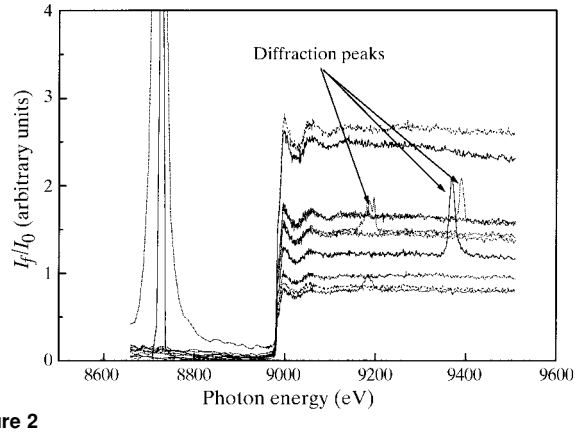

Figure 2
The fluorescence signals from each element of a 19-element solid-state detector (SSD). The sample is Cu/TiO_2 (110).

Table 1
Axis ranges and precision of the six-axis goniometer.

Axis	Range	Precision
θ	−5 to 140°	0.003°
ϕ	−3 to 3°	0.0004°
φ	−93 to 3°	0.005°
x	−10 to 10 mm	0.08 µm
y	−10 to 10 mm	0.08 µm
z	−10 to 10 mm	0.05 µm

2. *In situ* PTRF-XAFS system

To satisfy the above conditions (iv) and (v) at the same time, we constructed two separate ultra-high-vacuum (UHV) chambers, a sample-preparation chamber and a PTRF-XAFS measurement chamber, between which samples are transferred with a transfer chamber.

Fig. 1 illustrates the measurement chamber, the dimensions of which are 400 (width) × 400 (length) × 600 (height) mm and the base pressure of which is 10^{-10} torr (1 torr = 133.32 Pa). Reaction gases can be introduced through two leak valves and gas-phase analysis can be carried out by a quadrupole mass spectrometer (Q-mass; Balzers Co., Prisma). Incident and reflected X-rays pass through two Be windows (thickness 200 µm, diameter 14 mm, purity 99.8%). The beam size of the incident X-rays can be adjusted by selecting a series of Ta pinhole slits in front of the I_0 ionization chamber.

A multi-element SSD can be placed outside the chamber and the fluorescence signal is extracted through Be windows attached to the UHV flange. The positions of the Be windows are in line with those of the SSD windows in order to obtain maximum efficiency. The use of a multi-element SSD increases the solid angle and the maximum counting rates, as reported by Oyanagi & Nomura (Oyanagi *et al.*, 1998; Nomura, 1998). Moreover, the SSD can eliminate residual elastic scattering and fluorescence of the substrate and coexisting elements in order to increase the signal-to-background ratio. In the PTRF-XAFS measurement of a single-crystal substrate, diffracted beams from the substrate produce a discontinuity in the spectra at certain energies. Because the directionality of the diffracted beam is sharp, the diffraction line can be eliminated by an adequate adjustment of the detector position (Chun *et al.*, 1996). In the multi-element detection system, the diffracted beam can be easily removed by omitting the data of a few detector elements that suffer from the diffraction line, as shown in Fig. 2.

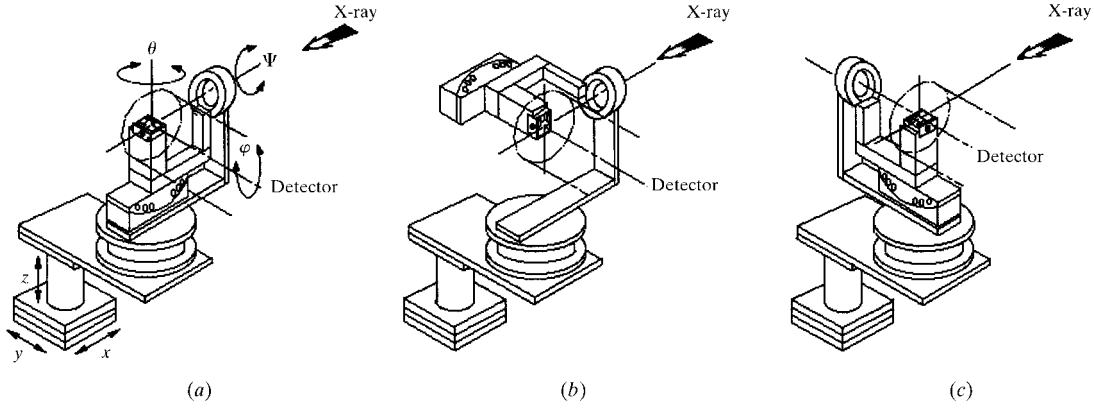

Figure 3
The high-precision UHV-compatible six-axis goniometer and its configuration for measurements against three different polarization directions: (*a*) *s*-polarization (**E** ∥ surface), (*b*) *p*-polarization (**E** ⊥ surface) and (*c*) the second *s*-polarization but perpendicular to the direction of (*a*).

The sample can be heated up to 600 K by resistive heating of W wire mounted in the sample holder. A ceramics block thermally and electrically isolates a goniometer from the sample holder.

To achieve total-reflection conditions precisely, we have used a UHV-compatible six-axis goniometer, as shown in Fig. 3. The goniometer is made of aluminium in order to lessen the weight load on the stepping motors. The rotation centre of the goniometer is fixed at that of the sample surface. Three (θ, φ and χ) rotation axes are driven by bake-proof vacuum stepping motors (Oriental Motors Co. UPX535M), while x, y and z motions are introduced from outside the chamber using usual stepping motors (Oriental Motors Co. UPD533HGI-NA, UPK564A-TG20). The range and precision for each axis are listed in Table 1.

Fig. 4 shows the X-ray reflectivity of the TiO_2 (110) surface at an energy of 9.3 keV. The critical angle was 3 mrad. The angle and the position could be reproduced even after a wide range of rotations and movements at room temperature. However, there was a small shift in the angle datum point when the sample was heated at elevated temperatures. The broken line in Fig. 4 represents the X-ray reflectivity of the same sample after heating at 473 K and cooling to room temperature in hydrogen atmosphere. The shift of the datum point was only 0.5 mrad. Therefore, one has to readjust the total-reflection conditions when the sample has been heated at a different temperature.

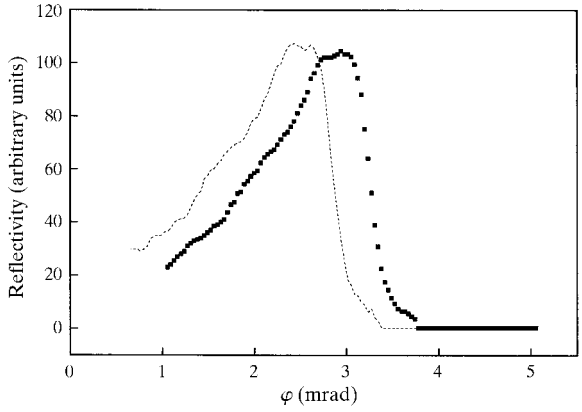

Figure 4
X-ray reflectivity of the TiO_2 (110) single crystal. The solid line and the broken line correspond to the reflectivities before and after heating the sample at 473 K, respectively.

Fig. 3 shows the setup of the goniometer for three different sample configurations, *i.e.* the electric vector perpendicular to the surface (*p*-polarization) and those parallel to the surface (*s*-polarization). If the surface symmetry is less than threefold, two directions parallel to the surface can be distinguished. For example, rutile TiO_2 (110) has different structures between the [001] and [1$\bar{1}$0] directions (Chun *et al.*, 1998).

Fig. 5 shows a perspective view of the preparation chamber. The UHV chamber [350 (width) × 350 (length) × 400 (height) mm] can be equipped with Q-Mass, LEED, AES and XPS (X-ray photoelectron spectroscopy) instruments. The base pressure is 10^{-10} torr. The substrate crystal can be cleaned by repeated Ar-ion sputtering and annealing cycles in the preparation chamber. A large crystal (more than 2 cm long) is required in order to increase the radiation area for grazing-incidence conditions. The sample can be completely covered with the mug-shaped heating module and annealed homogeneously up to 1000 K.

The prepared samples are then transferred to the measurement chamber using a small transfer chamber, which is also operated under UHV conditions. A non-evaporable getter pump is installed to maintain the high vacuum during the transfer of the sample from the preparation chamber to the measurement chamber in a beamline. The transfer chamber can contain two samples at the same time and thus the transfer chamber may be used as a 'parking lot' for the samples.

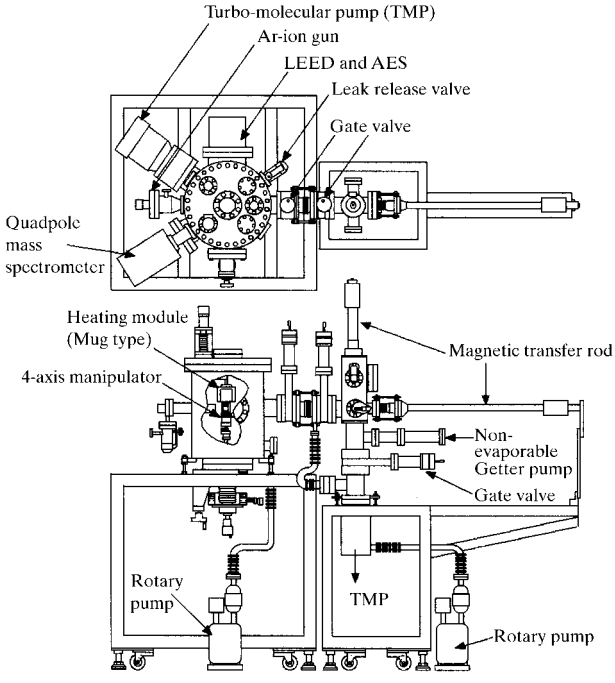

Figure 5
The sample-preparation chamber and the sample-transfer chamber.

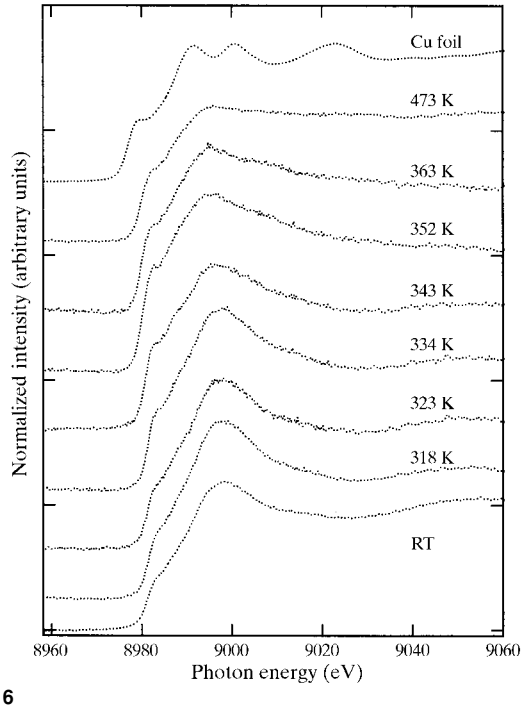

Figure 6
XANES spectra along [001] during the temperature-programmed reduction (TPR) process. RT = room temperature.

3. *In situ* PTRF-XAFS measurement of Cu particles on TiO_2 (110) derived from $Cu(DPM)_2$ as a precursor under temperature-programmed reduction

Cu/TiO_2 shows high activity in methanol synthesis by CO_2 hydrogenation and photocatalytic reduction of N_2O at room temperature. As a model of the Cu/TiO_2 catalyst, we deposited a Cu species on a TiO_2 (110) single crystal. We used $Cu(DPM)_2$ (DPM = 2,2,6,6-tetramethyl-3,5-heptanedione) as the precursor for the Cu species, which can be easily reduced at low temperature under H_2 atmosphere (Sekine *et al.*, 1992). Cu species were deposited on the TiO_2 (110) by dropwise addition of a diethyl ether solution of $Cu(DPM)_2$ under Ar flow. The remaining solvent was removed by evacuation for 24 h. The samples were then transferred to the measurement chamber.

Temperature-programmed reduction (TPR) was carried out in the measurement chamber at a rate of 8 K min^{-1} under 2 torr H_2. PTRF-XAFS spectra were measured at BL12C of the Photon Factory in the Institute of Material Structure Science, High Energy Accelerator Research Organization (KEK-PF) (Proposal No. 98 G305). The synchrotron radiation was monochromated by a Si (111) double-crystal monochromator. The storage ring was operated at 2.5 GeV and 200–400 mA. Cu *K*-edge EXAFS spectra were recorded in the range 8660–9500 eV at room temperature. The X-ray beam size was reduced to 0.4 mm in diameter in order to decrease unnecessary irradiation.

Cu *K*-edge XAFS measurements were carried out in three different directions of the electric vector of the incident X-rays, *i.e.* parallel to the [1$\bar{1}$0], [001] and [110] axes of TiO_2 (110). Fig. 6 shows the PTRF-XANES spectra parallel to the [001] direction during the TPR process. By increasing the reduction temperature, we observed that the pre-edge shoulder in the XANES spectra gradually increased up to 363 K. Fig. 7 shows the background-subtracted PTRF-EXAFS spectra of the sample treated at 363 K. $\chi(k)$ along the [001] axes showed different features compared with the behaviour in other directions. The detailed analysis of the EXAFS data will be discussed in another paper (Tanizawa *et al.*, 2001) but the EXAFS data clearly indicate the presence of anisotropic structure caused by the preferential formation of Cu—Cu bonds along the [001] direction of the TiO_2(110) support.

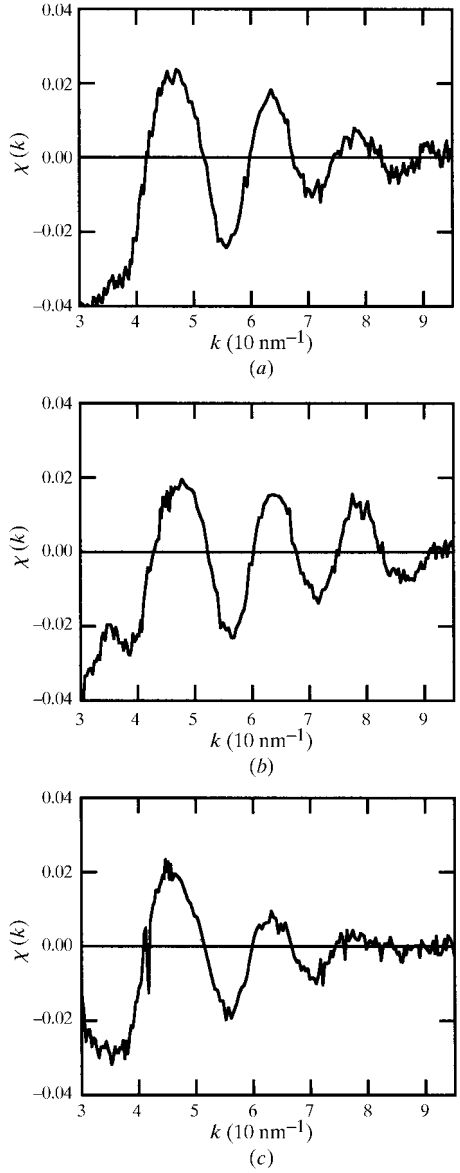

Figure 7
EXAFS oscillations for Cu/TiO_2 reduced at 363 K: (*a*) **E** || [1$\bar{1}$0], (*b*) **E** || [001], and (*c*) *E* || [110].

4. Conclusion

PTRF-XAFS has become a practical tool for the determination of the structure of the dispersed species on model single-crystal surfaces and enables us to start systematic investigations of metal–support interface structures.

This work has been supported by CREST (Core Research for Evolutional Science and Technology) of the Japan Science and Technology Corporation (JST) and performed under the approval of the Photon Factory Advisory Committee (Proposal No. 98G305).

References

Asakura, K., Chun, W.-J. & Iwasawa, Y. (2000). *Top. Catal.* **10**, 209–219.
Asakura, K., Chun, W.-J., Shirai, M., Tomishige, K. & Iwasawa, Y. (1997). *J. Phys. Chem. B*, **101**, 5549–5556.
Asakura, K., Shirai, M. & Iwasawa, Y. (1993). *Catal. Lett.* **20**, 117–124.
Asakura, K., Yamada, M., Iwasawa, Y. & Kuroda, H. (1985). *Chem. Lett.* pp. 511–514.
Chen, H. & Heald, S. M. (1993). *J. Appl. Phys.* **73**, 2467–2471.
Chun, W.-J., Asakura, K. & Iwasawa, Y. (1996). *J. Synchrotron Rad.* **3**, 160–162.
Chun, W.-J., Asakura, K. & Iwasawa, Y. (1998). *J. Phys. Chem. B*, **102**, 9006–9014.
Heald, S. M., Chen, H. & Tranquada, J. M. (1988). *Phys. Rev. B*, **38**, 1016–1026.
Heald, M., Keller, E. & Stern, E. A. (1984). *Phys. Lett.* **103A**, 155–158.
Iwasawa, Y. (1996). Editor. *X-ray Absorption Fine Structure for Catalysts and Surfaces*. Singapore: World Scientific.
Koningsberger, D. C. & Gates, B. C. (1992). *Catal. Lett.* **14**, 271–277.
Koningsberger, D. C. & Prins, R. (1988). Editors. *X-ray Absorption, Principles, Applications, Techniques of EXAFS, SEXAFS and XANES*. New York: John Wiley.
Koningsberger, D. C., van Zon, F. B. M., Vaarkamp, M. & Munoz-Paez, A. (1996). *X-ray Absorption Fine Structure for Catalysts and Surfaces*, edited by Y. Iwasawa, p. 257. Singapore: World Scientific.
Martens, J. H. A., Prins, R., Zanbergen, H. & Koningsberger, D. C. (1988). *J. Phys. Chem.* **92**, 1903–1916.
Nomura, M. (1998). *J. Synchrotron Rad.* **5**, 851–853.
Oyanagi, H., Martini, M. & Saito, M. (1998). *Nucl. Instrum. Methods*, **403**, 58–64.
Sekine, R., Kawai, M., Asakura, K., Hikita, T. & Kudo, M. (1992). *Surf. Sci.* **278**, 175–182.

Shirai, M., Asakura, K. & Iwasawa, Y. (1992). *Chem. Lett.* pp. 1037–1040.
Shirai, M., Asakura, K. & Iwasawa, Y. (1994). *Catal. Lett.* **26**, 229–234.
Shirai, M., Inoue, T., Onishi, H., Asakura, K. & Iwasawa, Y. (1994). *J. Catal.* **145**, 159–164.
Shirai, M. & Iwasawa, Y. (1996). *X-ray Absorption Fine Structure for Catalysts and Surfaces*, edited by Y. Iwasawa, p. 332. Singapore: World Scientific.
Shirai, M., Nomura, M., Asakura, K. & Iwasawa, Y. (1995). *Rev. Sci. Instrum.* **66**, 5493–5498.
Tanizawa, Y., Chun, W.-J., Shido, T., Asakura, K. & Iwasawa, Y. (2001). *J. Synchrotron Rad.* **8**, pp. 508–510.
Zon, J. B. A. D. van, Koningsberger, D. C., van't Blik, H. F. J., Prins, R. & Sayers, D. E. (1984). *J. Chem. Phys.* **80**, 3914–3915.

 Received 26 July 2000 • Accepted 7 November 2000